

GST-tagged proteins using a pGEX 4T vector (Pharmacia). Full-length XIAP, BIR3 and mutant BIR3 were *in vitro* translated in the presence of <sup>35</sup>S-methionine in reticulocyte lysates using MYC-pcDNA3 vector. Smac, caspase-9-p12, p10 and linker peptide were overexpressed in *E. coli* strain BL21(DE3) as C-terminally GST-tagged proteins using a pET-28-GST vector. Apaf-1L was expressed in Sf-9 insect cells and purified to homogeneity as previously described<sup>14</sup>.

## Reconstitution and assay of the activity of the caspase-9–Apaf-1 holoenzyme complexes

Recombinant WT and mutant caspase-9 proteins (20 nM) were incubated in the presence or absence of recombinant Apaf-1 (20 nM) in buffer A<sup>6</sup>. The reaction mixtures were stimulated with cytochrome *c* (5 ng μl<sup>-1</sup>) and dATP (1 mM) and incubated for 0–60 min at 30 °C with purified procaspase-3 C163A, and the processing of procaspase-3 was analysed by western blot analysis with anti-caspase-3 antibody (Fig. 1c). The holoenzyme complexes were also reconstituted as above in caspase-9-depleted S100 extracts from Apaf-1-deficient mouse embryonic fibroblasts (Fig. 1d). The DEVD-AMC cleaving activity of the reconstituted extracts were measured over a time of 0–120 min by luminescence spectrometry and represented in arbitrary spectrometric units. In some experiments the WT and the unprocessed triple-mutant (E306/D315/330A) caspase-9 proteins (specific activity ~10 fluorogenic units per μg) were reconstituted with Apaf-1 and cytochrome *c* plus dATP in the presence of increasing amounts of XIAP, and the cleavage of <sup>35</sup>S-labelled procaspase-3 by the complexes was analysed by SDS-PAGE and autoradiography (Fig. 2a).

## Gel-filtration analysis of the caspase-9–Apaf-1 holoenzyme complexes

These procedures were performed as described before<sup>14</sup>. Caspase-9–Apaf-1 holoenzyme complexes containing WT or mutant caspase-9 were reconstituted in the presence of cytochrome *c* (5 ng μl<sup>-1</sup>) and dATP (1 mM) in oligomerization buffer I (25 mM HEPES (pH 7.4), 50 mM NaCl, 10 mM KCl, 5 mM MgCl<sub>2</sub>, 100 μg ml<sup>-1</sup> BSA, 5% glycerol, and 0.1 mM DTT) for 1 h at 30 °C. After incubation, the reaction mixtures were diluted with oligomerization buffer I and aliquots of each sample (100 μl) were loaded onto Superose-6 FPLC column. Equal volumes of the column fractions (50 μl) were separated by SDS-PAGE and immunoblotted with anti-Apaf-1 and anti caspase-9. In some experiments, the holoenzyme complexes were reconstituted in the presence of XIAP (Fig. 2b).

## Far-western blotting

Affinity purified proteins were subjected to SDS-PAGE and were transferred to nitrocellulose membrane using standard western blotting techniques. The proteins on the membrane were denatured in a buffer (10 mM sodium phosphate pH 7.4, 150 mM sodium chloride, 5 mM magnesium chloride and 1 mM DTT) containing 6 M guanidine-HCl. The proteins were renatured by gradual reduction of guanidine-HCl to 0.3 M. The membrane was blocked overnight in the same buffer containing 5% non-fat dry milk and then incubated with <sup>35</sup>S-labelled *in vitro* translated XIAP in the same buffer with 1% non-fat dry milk. The membrane was washed at least three times and then exposed to X-ray film.

## In vitro interaction assays

All *in vitro* interactions were performed as described<sup>6</sup>.

## Determination of IC<sub>50</sub>

WT caspase-3 or caspase-3 mutant proteins (10 pM) were incubated with purified BIR3 (0.5–800 nM) or BIR1-BIR2 proteins (0.1–80 nM) at 37 °C in the presence of DEVD-AMC (100 μM) for 30 min and the substrate cleavage was measured by luminescence spectrometry. The IC<sub>50</sub> values were then calculated using Graphpad Prism V2.0 (Graphpad Prism Software, San Diego, CA).

## DEVD cleavage assays

Caspase-3 enzymatic assays with the tetrapeptide substrate DEVD-AMC were performed as described<sup>6</sup>.

## Computer modelling

On the basis of the crystal structure of a Smac–BIR3 complex<sup>13</sup>, the N-terminal tetrapeptide of Smac was replaced by that from the p12 subunit of human caspase-9. Then we performed limited energy minimization on the complex between BIR3 and the tetrapeptide from the p12 subunit of the human caspase-9.

Received 4 December 2000; accepted 1 February 2001.

- Deveraux, Q. L. *et al.* Cleavage of human inhibitor of apoptosis protein XIAP results in fragments with distinct specificities for caspases. *EMBO J.* **18**, 5242–5251 (1999).
- Sun, C. *et al.* NMR structure and mutagenesis of the third BIR domain of the inhibitor of apoptosis protein XIAP. *J. Biol. Chem.* **275**, 33777–33781 (2000).
- Datta, R. *et al.* XIAP regulates DNA damage-induced apoptosis downstream of caspase-9 cleavage. *J. Biol. Chem.* **275**, 31733–31738 (2000).
- Verhagen, A. M. *et al.* Identification of DIABLO, a mammalian protein that promotes apoptosis by binding to and antagonizing IAP proteins. *Cell* **102**, 43–53 (2000).
- Du, C., Fang, M., Li, Y., Li, L. & Wang, X. Smac, a mitochondrial protein that promotes cytochrome *c*-dependent caspase activation by eliminating IAP inhibition. *Cell* **102**, 33–42 (2000).
- Srinivasula, S. M. *et al.* Molecular determinants of the caspase-promoting activity of Smac/DIABLO and its role in the death receptor pathway. *J. Biol. Chem.* **275**, 36152–36157 (2000).

- Chai, J. *et al.* Structural and biochemical basis of apoptotic activation by Smac/DIABLO. *Nature* **406**, 855–862 (2000).
- Abrams, J. M. An emerging blueprint for apoptosis in *Drosophila*. *Trends Cell. Biol.* **9**, 435–440 (1999).
- Chen, P., Nordstrom, W., Gish, B. & Abrams, J. M. Grim, a novel cell death gene in *Drosophila*. *Genes Dev.* **10**, 1773–1782 (1996).
- Srinivasula, S. M., Ahmad, M., Fernandes-Alnemri, T. & Alnemri, E. S. Autoactivation of procaspase-9 by Apaf-1-mediated oligomerization. *Mol. Cell* **1**, 949–957 (1998).
- Liu, Z. *et al.* Structural basis for binding of Smac/DIABLO to the XIAP BIR3 domain. *Nature* **408**, 1004–1008 (2000).
- Rodriguez, J. & Lazebnik, Y. Caspase-9 and APAF-1 form an active holoenzyme. *Genes Dev.* **13**, 3179–3184 (1999).
- Wu, G. *et al.* Structural basis of IAP recognition by Smac/DIABLO. *Nature* **408**, 1008–1012 (2000).
- Saleh, A., Srinivasula, S. M., Acharya, S., Fishel, R. & Alnemri, E. S. Cytochrome *c* and dATP-mediated oligomerization of Apaf-1 is a prerequisite for procaspase-9 activation. *J. Biol. Chem.* **274**, 17941–17945 (1999).

## Acknowledgements

We thank R. Penn for help with calculating IC<sub>50</sub> values. This work was supported by the NIH (E.S.A., P.D.R., Y.S.). S.M.S. is a special fellow of the Leukemia and Lymphoma Society; Y.S. is a Searle scholar and a Rita Allen scholar.

Correspondence and requests for materials should be addressed to E.S.A. (e-mail: E\_Alnemri@lac.jci.tju.edu).

# Methylation of histone H3 lysine 9 creates a binding site for HP1 proteins

Monika Lachner\*, Dónal O'Carroll\*, Stephen Rea, Karl Mechtler & Thomas Jenuwein

Research Institute of Molecular Pathology (IMP), The Vienna Biocenter, Dr Bohrgasse 7, A-1030 Vienna, Austria

\* These authors contributed equally to this work

Distinct modifications of histone amino termini, such as acetylation, phosphorylation and methylation, have been proposed to underlie a chromatin-based regulatory mechanism<sup>1,2</sup> that modulates the accessibility of genetic information. In addition to histone modifications that facilitate gene activity, it is of similar importance to restrict inappropriate gene expression<sup>3,4</sup> if cellular and developmental programmes are to proceed unperturbed. Here we show that mammalian methyltransferases that selectively methylate histone H3 on lysine 9 (Suv39h HMTases)<sup>5</sup> generate a binding site for HP1 proteins—a family of heterochromatic adaptor molecules<sup>6,7</sup> implicated in both gene silencing and supra-nucleosomal chromatin structure. High-affinity *in vitro* recognition of a methylated histone H3 peptide by HP1 requires a functional chromo domain; thus, the HP1 chromo domain is a specific interaction motif for the methyl epitope on lysine 9 of histone H3. *In vivo*, heterochromatin association of HP1 proteins is lost in *Suv39h* double-null primary mouse fibroblasts but is restored after the re-introduction of a catalytically active SUV39H1 HMTase. Our data define a molecular mechanism through which the SUV39H–HP1 methylation system can contribute to the propagation of heterochromatic subdomains in native chromatin.

The 'histone code' hypothesis<sup>1,2</sup> predicts that distinct modifications of the histone N termini can regulate interaction affinities for chromatin-associated proteins, similar to the binding of transcription factors to specific DNA sequences. For example, the acetylation of histone H4 tails induces an increased affinity for bromo-domain proteins<sup>8</sup>, thereby recruiting histone acetyltransferases (HATs) to nucleosomal regions of transcriptional activity. The human (SUV39H1) or murine (Suv39h1) histone

methyltransferases (HMTases) and their associated HP1 proteins<sup>9</sup> share the evolutionarily highly conserved chromo domain<sup>10,11</sup>, which has been implicated in directing euchromatic or heterochromatic localizations<sup>12</sup>. On the basis of these intriguing parallels, we reasoned that the SUV39H1-dependent methylation of lysine 9 in H3 (ref. 5) may generate a specific binding surface for either the HMTase itself or for the associated HP1 protein(s).

To investigate directly whether SUV39H1 or HP1 proteins could display affinity for the H3 N terminus, we developed an *in vitro* 'pull-down assay' by covalently coupling unmodified, Lys-9-dimethylated (K9-dimeth) and Ser-10-phosphorylated (S10-phos) H3 N-terminal peptides (residues 1–20) to an affinity matrix (see Methods). As a control, we also prepared a matrix presenting an unmodified H4 N-terminal peptide (residues 1–20). Triple Myc-tagged complementary DNAs of human SUV39H1 and murine HP1 $\alpha$ , HP1 $\beta$  and HP1 $\gamma$  were *in vitro* translated, and recombinant proteins were incubated with a 1,000-fold or greater excess (see Methods) of the different covalently attached histone N-terminal peptides. After extensive washing, bound proteins were visualized by protein blot analysis with anti-Myc antibodies. To compare binding specificities, we also included the transcription factor Pax5 (ref. 13) and the murine Polycomb group protein mPC1 (ref. 14) in this analysis (Fig. 1a, b). The *Drosophila* Polycomb<sup>15</sup> and HP1 (ref. 16) proteins have been shown to interact with histones *in vitro*.

Whereas (Myc)<sub>3</sub>-Pax5 did not display binding to any of the matrices, (Myc)<sub>3</sub>-mPC1 showed nonspecific associations. Similarly, although binding of (Myc)<sub>3</sub>-SUV39H1 was slightly enhanced with the K9-dimeth peptide, it was also retained with all of the other N termini. In contrast, the three (Myc)<sub>3</sub>-HP1 proteins only reacted with the K9-dimeth peptide (Fig. 1c, lower panels) but did not display associations with unmodified H3, or the S10-phos or H4 peptides.

HP1 proteins are characterized by the evolutionarily conserved chromo domain<sup>10,11</sup> and by a related carboxy-terminal shadow

domain that directs intra- and intermolecular interactions<sup>6,7</sup>. To examine the domain requirements for association with the H3 Lys 9 N terminus, we introduced point mutations (V23M or V26R) in the first  $\beta$ -sheet of the HP1 $\beta$  chromo domain that would interfere with a predicted hydrophobic binding pocket<sup>12</sup>. We also generated truncated (Myc)<sub>3</sub>-HP1 $\beta$  proteins that comprise only the chromo (residues 4–96) or the shadow (residues 110–185) domain (Fig. 2a). Quantitative pull-down assays with full-length HP1 $\beta$  indicated that saturated binding occurred with a 500- to 10,000-fold excess of the H3 K9-dimeth peptide. By contrast, both chromo point mutants displayed impaired affinity and the shadow domain showed no interaction at all (Fig. 2b). Notably, the isolated HP1 $\beta$  chromo domain can recognize the H3 Lys 9 methylation mark, although its binding requires a 10- to 20-fold increase in the concentration of the H3 K9-dimeth peptide as compared with full-length HP1 $\beta$ .

To validate these findings, we next examined the relative ratios at which free peptide would compete away full-length HP1 $\beta$  or the isolated HP1 $\beta$  chromo domain from the affinity matrix. We bound about 20 ng of (Myc)<sub>3</sub>-HP1 $\beta$  or (Myc)<sub>3</sub>-chromo to the H3 K9-dimeth matrix and then incubated with increasing concentrations (10-fold increments) of either unmodified or K9-dimeth H3 peptides. Whereas the unmodified H3 peptide was inactive over the entire concentration range, a 10,000-fold excess of the K9-dimeth H3 peptide was required to dissociate (Myc)<sub>3</sub>-HP1 $\beta$  (Fig. 2c). By contrast, the affinity of (Myc)<sub>3</sub>-chromo was significantly weaker; this domain had already eluted at a 1,000-fold excess of the K9-dimeth H3 peptide. Together with the above results, these data indicate that the HP1 $\beta$  chromo domain interacts with the H3 Lys9 methylation mark *in vitro*; however, they further suggest that full-length HP1 $\beta$  or an HP1 $\beta$  dimer<sup>17</sup> is necessary for high-affinity binding. The latter interpretation is particularly intriguing because it would allow many interactions to occur between Lys-9-dimethylated H3 N termini and dimerized HP1 molecules, thereby stabilizing their binding.

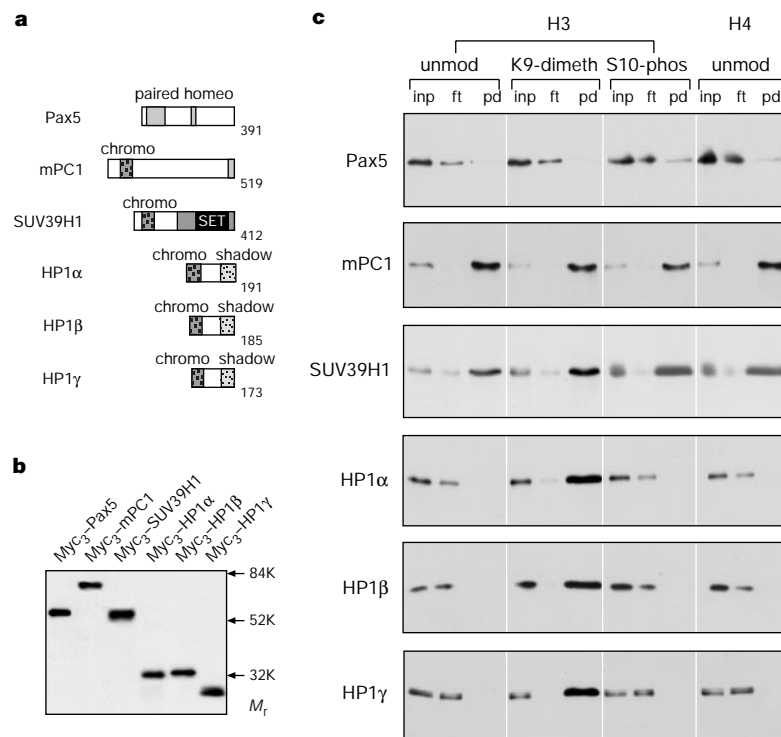


**Figure 1** The H3 Lys9 methyl epitope activates a specific binding site for HP1 proteins *in vitro*. **a**, Diagram of the domain structures of murine Pax5, murine mPC1, human SUV39H1 and murine HP1 $\alpha$ , HP1 $\beta$  and HP1 $\gamma$ . **b**, Protein blot of *in vitro* translated and pre-calibrated (Myc)<sub>3</sub>-tagged proteins detected by anti-Myc antibodies. **c**, *In vitro* pull-

down assays with the indicated (Myc)<sub>3</sub>-tagged proteins on affinity matrices that present either unmodified (unmod), Lys-9-dimethylated (K9-dimeth) and Ser10-phosphorylated (S10-phos) H3 N-terminal peptides, or an unmodified H4 N terminus. 'inp', 10% of IVT proteins used for binding; 'ft', 10% of flow-through; 'pd', pulled-down (bound proteins).

To show that H3 Lys 9 methylation is also the crucial determinant for HP1 localization in native chromatin, we next analysed the nuclear distribution of HP1 proteins in wild-type versus mutant primary mouse embryonic fibroblasts (PMEFs) in which the two murine *Suv39h* genes had been disrupted<sup>5</sup>. Mammalian HP1 proteins are enriched at heterochromatic foci<sup>18,19</sup>, which can readily be visualized in mouse cells by counterstaining of (A+T)-rich repeat sequences with 4',6-diamidino-2-phenylindole (DAPI). Heterochromatic association of murine HP1 proteins was unaltered only if single *Suv39h1* or *Suv39h2* gene disruptions were introduced into PMEFs (data not shown; for wild-type localization see below). By contrast, indirect immunofluorescence for HP1 $\beta$  or HP1 $\alpha$  epitopes in interphase chromatin of *Suv39h* double-null PMEFs indicated that both proteins are dispersed from heterochromatin. These results are consistent with complementary analyses of *clr4* mutants in *Schizosaccharomyces pombe*<sup>20</sup>.

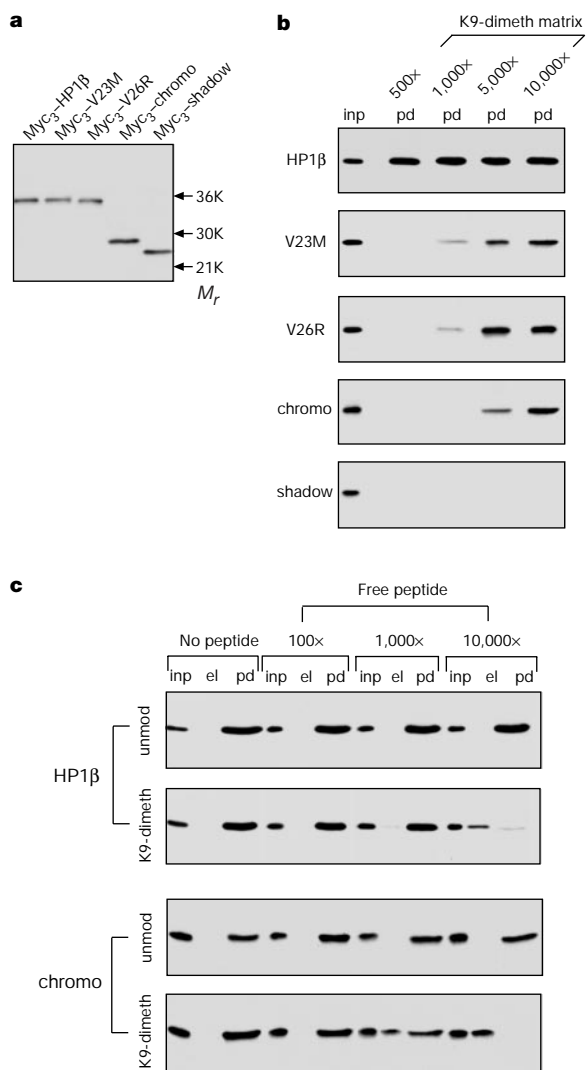


**Figure 2** Mutant analysis of HP1 $\beta$  and quantitation of *in vitro* binding to the H3 K9-dimeth peptide matrix. **a**, Protein blot of *in vitro* translated and pre-calibrated (Myc)<sub>3</sub>-tagged HP1 $\beta$  mutant proteins detected by anti-Myc antibodies. **b**, Quantitative pull-down assays of (Myc)<sub>3</sub>-tagged HP1 $\beta$  mutants with the H3 K9-dimeth affinity matrix. Binding was analysed with ~20 ng of IVT proteins and increasing concentrations of H3 K9-dimeth N termini (indicated as fold excess). **c**, Quantitative elution of pre-bound (Myc)<sub>3</sub>-HP1 $\beta$  and (Myc)<sub>3</sub>-chromo with increasing concentrations (indicated as fold excess) of unmodified or K9-dimeth H3 N-terminal peptides. 'inp', 10% of pre-bound proteins; 'el', 20% of first wash; 'pd', pulled down (proteins retained on matrix after final washes).

To determine more definitively that HP1 localization is dependent on Suv39h-mediated HMTase activity and not on association with Suv39h proteins<sup>9,21</sup>, we re-introduced an active human (Myc)<sub>3</sub>-SUV39H1 HMTase or a catalytically inactive (Myc)<sub>3</sub>-SUV39H1 mutant (H324L)<sup>5</sup> into wild-type and *Suv39h* double-null PMEFs by retroviral infection. Expression of a linked green fluorescent protein (GFP) indicated 80–90% infection efficiency (see Methods; data not shown). Protein blot analysis with nuclear extracts from infected cells confirmed a comparable abundance of ectopic proteins (Fig. 3a), and catalytic activity or inactivity (of the H324L mutant) was shown by HMTase assays after immunoprecipitation with anti-Myc antibodies (Fig. 3b).

We then examined nuclear localization of ectopic SUV39H1 proteins in wild-type PMEFs by indirect immunofluorescence with anti-Myc antibodies. Whereas mock-infected cells were Myc negative, both (Myc)<sub>3</sub>-SUV39H1 and the (Myc)<sub>3</sub>-SUV1(H324L) mutant are enriched at heterochromatic foci, in a staining that largely overlaps with colocalized HP1 $\beta$  and HP1 $\alpha$  (Fig. 4, right panels). This result indicates that heterochromatin association of SUV39H1 in a wild-type background can be uncoupled from its intrinsic HMTase activity, and is consistent with our previous structure–function analysis that defined a heterochromatin targeting and HP1 $\beta$  interaction domain at the N terminus of SUV39H1 (ref. 21).

Finally, we colocalized ectopic SUV39H1 and endogenous HP1 $\beta$  and HP1 $\alpha$  proteins in infected *Suv39h* double-null PMEFs. In contrast to wild-type cells, the (Myc)<sub>3</sub>-SUV1(H324L) mutant only displayed diffuse nuclear staining, similar to the dispersed distribution of endogenous HP1 proteins (Fig. 4, left panel). Notably, the catalytically active (Myc)<sub>3</sub>-SUV39H1 HMTase was enriched at heterochromatin and could induce relocalization of

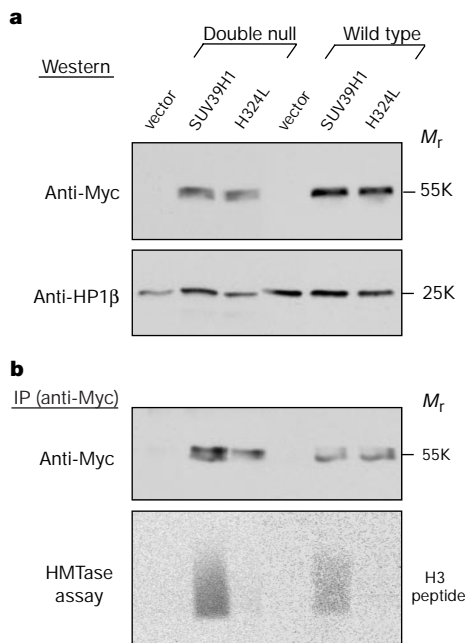


**Figure 3** Characterization of transduced SUV39H1 HMTase activity in PMEFs. **a**, Protein blot analysis with 30  $\mu$ g of nuclear extracts from wild-type and *Suv39h* double-null mouse primary embryonic fibroblasts (PMEFs) that had been mock-infected (vector) or productively infected with retroviruses carrying an active ('SUV39H1', (Myc)<sub>3</sub>-SUV39H1) or an inactive ('H324L', (Myc)<sub>3</sub>-SUV1(H324L)) HMTase. As a loading control and to demonstrate similar abundance of endogenous HP1 proteins, the blot was cut and also probed with antibodies specific for HP1 $\beta$ . **b**, HMTase assay with an N-terminal H3 peptide and transduced (Myc)<sub>3</sub>-SUV39H1 enzymes that were enriched by immunoprecipitation (IP) from 500  $\mu$ g of nuclear PMEF extracts with anti-Myc antibodies.

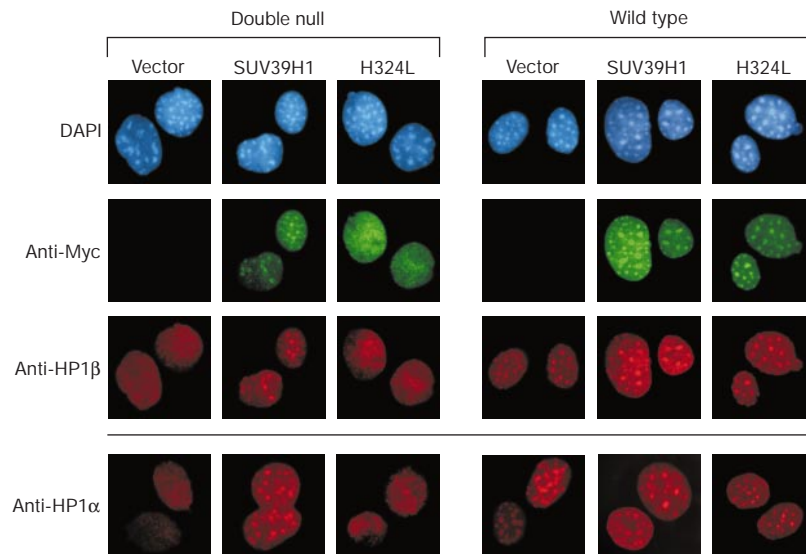


**Figure 4** Rescue of heterochromatic localization of HP1 proteins by an active SUV39H1 HMTase. Double-label indirect immunofluorescence of wild-type (right panel) and *Suv39h* double-null (left panel) PMEFs that had been infected with (Myc)<sub>3</sub>-SUV39H1-transducing retroviruses as in Fig. 3. Expression analysis of a linked GFP protein indicated 80–90% infection efficiency (data not shown). Mouse interphase chromatin was co-stained with

anti-Myc (green) and anti-HP1β antibodies (red). DNA was counterstained with DAPI (blue). In additional samples, PMEF interphase chromatin was co-stained with anti-Myc (not shown) and anti-HP1α antibodies (red). Contrast of images was adjusted with Adobe Photoshop 4.0.

HP1β and HP1α to these heterochromatic foci (Fig. 4, middle row, left panel). Together, these results strongly suggest that the Suv39h-dependent methylation of Lys 9 in H3 (ref. 3) transduces the signal to recruit the SUV39H–HP1 complex to heterochromatic regions in mammalian chromatin.

In contrast to gene activity controlled by sequence-specific transcription factors, epigenetic mechanisms for variegating gene expression have been difficult to define at a molecular level, because it remained unclear how they would discriminate target loci for activation or repression<sup>22–25</sup>. The Suv39h HMTases selectively methylate H3 at Lys 9, and their activity is impaired by pre-existing modifications in the H3 N terminus<sup>5</sup>. Thus, conditions that entail the presentation and incorporation of unmodified H3 tails, for example, decaying transcriptional activity during developmental programmes<sup>26</sup> or replication-coupled histone deposition<sup>27,28</sup> at transcriptionally non-permissive regions, are likely to favour the establishment of the Suv39h-dependent H3 Lys 9 methyl epitope. Moreover, because Lys 9 in H3 can either be methylated or acetylated<sup>1,29</sup>, competitive modification of this position could provide a molecular ‘switch’ for the induction of euchromatic or heterochromatic subdomains, if the activity or abundance of the respective enzymes is altered. For example, forced overexpression of SUV39H1 induces ectopic heterochromatin by redistributing endogenous HP1β<sup>21</sup>. On the basis of our data, we propose that the SUV39H–HP1 methylation system contributes to higher order chromatin organization by propagating a heterochromatin-specific affinity in the histone H3 N terminus. □

## Methods

### *In vitro* translation of (Myc)<sub>3</sub>-tagged proteins

A (Myc)<sub>3</sub>-H6 epitope including a unique *NotI* cloning site was inserted into the polylinker of pKW2T, which allows *in vitro* transcription by the SP6 RNA polymerase. The plasmid for parental (Myc)<sub>3</sub>-SUV39H1 (residues 3–412) has been described<sup>9</sup>. Additional (Myc)<sub>3</sub>-tagged proteins were generated by transferring *NotI/EcoRI* polymerase chain reaction (PCR) amplicons into the pKW2T derivative, encoding in-frame fusions for Pax5 (residues 4–391)<sup>13</sup>, mPC1 (residues 3–519)<sup>14</sup>, HP1α (residues 5–191), HP1β (residues 5–185), HP1γ (residues 5–173) and the HP1β chromo (residues 4–96) or HP1β shadow (residues 110–185) domain<sup>7,11,17</sup>. The V23M and V26R point mutations were directly generated in the (Myc)<sub>3</sub>-HP1β construct by double PCR mutagenesis. All plasmids were confirmed by sequencing, which detected the presence of a point mutation (G8A) in

mPC1 and of another point mutation (D65A) in HP1γ.

Plasmid DNA (1 μg) was transcribed and translated (TNT-kit; Promega) in a volume of 50 μl, and *in vitro* translated (IVT) proteins were calibrated by immunoblotting with anti-Myc antibodies visualized by peroxidase staining using enhanced chemiluminescence (ECL; Amersham).

### *In vitro* pull-down assays with peptide matrices

Affinity matrices were generated in 400 μl of HEPES pH 7.9 by covalently coupling, for 2 h at room temperature, 1.4 mg of histone peptides (~600 nmol) through a C-terminal cysteine to 5 mg of activated Poros beads (Applied Biosystems), representing ~300 nmol of active maleimid groups through the bifunctional crosslinker sulfo-GMBS (Pierce). Saturation of the matrices was determined by the 412-nm absorbance of free thiol-groups using 5,5'-dithio-bis (2-nitrobenzoic acid) (Sigma). Matrices can be stored at 4 °C.

The unmodified H3 N-terminal (residues 1–20), K9-dimeth and S10-phos H3 peptides have been described<sup>5</sup>. In addition, we also prepared an affinity matrix with the N terminus of histone H4 (SGRGKGGKGLGKGGAKRHRK-Cys).

*In vitro* pull-down assays were modified on the basis of described protocols<sup>30</sup> with a ≈ 1,000-fold excess of N termini over IVT proteins. For one *in vitro* reaction, 10 μl of the peptide matrices (≤ 1 nmol of covalently attached peptide) were washed three times in binding buffer (20 mM Tris pH 8, 150 mM NaCl, 1 mM EDTA, 0.1% Triton X-100) before incubation with 2–10 μl of IVT proteins (~1 pmol or 20 ng of recombinant protein) in a volume of 170 μl for 60 min at room temperature. Reactions were vigorously washed five times in 50 mM HEPES pH 7.5, 0.5 M NaCl, 1 mM EDTA, 1% NP-40, and bound proteins were eluted in SDS sample buffer, separated by 10 or 12% SDS-PAGE and visualized by immunoblotting with anti-Myc antibodies.

For the elution analysis, eight aliquots of 20 ng IVT proteins were bound for 1 h at room temperature under saturating conditions to 10 μl ((Myc)<sub>3</sub>-HP1β) or 100 μl ((Myc)<sub>3</sub>-chromo) of the K9-dimeth matrix and washed twice. Loaded matrices were then incubated for an additional 1 h at room temperature in 150 μl of binding buffer containing increasing concentrations of free peptides, washed five times and analysed as above.

### Analysis and rescue of PMEFs

PMEFs were derived from embryonic day E12.5 *Suv39h* double-null fetuses obtained after intercrossing *Suv39h1*<sup>-/-</sup>/*Suv39h2*<sup>+/-</sup> compound mutant mice (D. O’C. *et al.*, manuscript in preparation). As controls, PMEFs were prepared from wild-type fetuses of the same genetic background. Co-staining of Triton X-100 extracted PMEF interphase chromatin was performed with rat monoclonal anti-HP1β<sup>18</sup> and mouse monoclonal anti-Myc (9E10) antibodies, or with mouse monoclonal anti-HP1α (Piere Chambon, Illkirch) and rabbit polyclonal anti-Myc (9E10) (Lukas Huber, IMP) antibodies, followed by counterstaining of DNA with 4',6'-diamidino-2-phenylindole (DAPI; Sigma) as described<sup>21</sup>.

For the rescue experiment, the H324L mutation<sup>5</sup> was introduced into full-length (Myc)<sub>3</sub>-SUV39H1, and (Myc)<sub>3</sub>-SUV39H1 and (Myc)<sub>3</sub>-SUV1(H324L) *SalI/EcoRI* DNA fragments were transferred into the polylinker of MSCV-MIGR1 (a derivative of murine stem-cell virus plasmid; Clontech) that contains a linked humanized IRES-GFP protein instead of PGK-*neo*. SUV1 plasmids and empty MSCV-MIGR1 vector were transiently transfected into the ecotropic φNX-eco helper-free packaging cell line (G. Nolan, Stanford). Passage 3 wild-type and *Suv39h* double-null PMEFs (3 × 10<sup>5</sup> cells per 10-cm dish) were infected twice with φNX virus S/N, and cells were grown for 3 d before analysis

of GFP expression, indirect immunofluorescence, ectopic protein abundance and HMTase assay<sup>3</sup>.

Received 9 November; accepted 8 December 2000.

1. Strahl, B. D. & Allis, C. D. The language of covalent histone modifications. *Nature* **403**, 41–45 (2000).
2. Turner, B. M. Histone acetylation and an epigenetic code. *BioEssays* **22**, 836–845 (2000).
3. Paro, R. & Harte, P. J. in *Epigenetic Mechanisms of Gene Regulation* (eds Russo, V. A. E., Martienssen, R. A. & Riggs, A. D.) 507–528 (CSHL, New York, 1996).
4. Pirrotta, V. Polycomb: the genome: PcG, trxG, and chromatin silencing. *Cell* **93**, 333–336 (1998).
5. Rea, S. *et al.* Regulation of chromatin structure by site-specific histone H3 methyltransferases. *Nature* **406**, 593–599 (2000).
6. Wallrath, L. L. Unfolding the mysteries of heterochromatin. *Curr. Opin. Genet. Dev.* **8**, 147–153 (1998).
7. Jones, D. A., Cowell, I. G. & Singh, P. B. Mammalian chromodomain proteins: their role in genome organisation and expression. *BioEssays* **22**, 124–127 (2000).
8. Jacobson, R. H., Ladurner, A. G., King, D. S. & Tjian, R. Structure and function of a human TAF<sub>II</sub>250 double bromodomain module. *Science*, **288**, 1422–1425 (2000).
9. Aagaard, L. *et al.* Functional mammalian homologues of the *Drosophila* PEV modifier *Su(var)3–9* encode centromere-associated proteins which complex with the heterochromatin component M31. *EMBO J.* **18**, 1923–1938 (1999).
10. Paro, R. & Hogness, D. S. The Polycomb protein shares a homologous domain with a heterochromatin-associated protein of *Drosophila*. *Proc. Natl Acad. Sci. USA* **88**, 263–267 (1991).
11. Ball, L. J. *et al.* Structure of the chromatin binding (chromo) domain from mouse modifier protein 1. *EMBO J.* **16**, 2473–2481 (1997).
12. Platero, J. S., Harnett, T. & Eisenberg, J. C. Functional analysis of the chromodomain of *HP-1*. *EMBO J.* **14**, 3977–3986 (1995).
13. Adams, B. *et al.* *Pax-5* encodes the transcription factor BSAP and is expressed in B lymphocytes, the developing CNS, and adult testis. *Genes Dev.* **6**, 1589–1607 (1992).
14. Pierce, J. J., Singh, P. B. & Gaunt, S. J. The mouse has a polycomb-like chromobox gene. *Development* **114**, 921–929 (1992).
15. Breiling, A., Bonte, E., Ferrari, S., Becker, P. B. & Paro, R. The *Drosophila* Polycomb protein interacts with nucleosomal core particles *in vitro* via its repression domain. *Mol. Cell. Biol.* **19**, 8451–8460 (1999).
16. Zhao, T., Heyduk, T., Allis, C. D. & Eisenberg, J. C. Heterochromatin protein 1 (HP1) binds to nucleosomes and DNA *in vitro*. *J. Biol. Chem.* **275**, 28332–28338 (2000).
17. Brasher, S. V. *et al.* The structure of mouse HP1 suggests a unique mode of single peptide recognition by the shadow chromo domain dimer. *EMBO J.* **19**, 1587–1597 (2000).
18. Wreggett, K. A., Hill, E., James, P. S., Hutchings, G. W. & Singh, P. B. A mammalian homologue of *Drosophila* heterochromatin protein 1 (HP1) is a component of constitutive heterochromatin. *Cytogenet. Cell Genet.* **66**, 99–103 (1994).
19. Minc, E., Allory, Y., Worman, H. J., Courvalin, J.-C. & Buendia, B. Localization and phosphorylation of HP1 proteins during the cell cycle in mammalian cells. *Chromosoma* **108**, 220–234 (1999).
20. Ekwall, K. *et al.* Mutations in the fission yeast silencing factors *clr4<sup>+</sup>* and *rik1<sup>+</sup>* disrupt the localisation of the chromo domain protein Swi6p and impair centromere function. *J. Cell Sci.* **109**, 2637–2648 (1996).
21. Melcher, M. *et al.* Structure–function analysis of SUV39H1 reveals a dominant role in heterochromatin organization, chromosome segregation and mitotic progression. *Mol. Cell. Biol.* **20**, 3728–3741 (2000).
22. Grosveld, F. Activation by locus control regions? *Curr. Opin. Genet. Dev.* **9**, 152–157 (1999).
23. Festenstein, R. *et al.* Heterochromatin protein 1 modifies mammalian PEV in a dose- and chromosomal context-dependent manner. *Nature Genet.* **23**, 457–461 (1999).
24. Nielsen, A. L. *et al.* Interaction with members of the heterochromatin protein 1 (HP1) family and histone deacetylation are differentially involved in transcriptional silencing by members of the TIF1 family. *EMBO J.* **18**, 6385–6395 (1999).
25. Ryan, R. F. *et al.* KAP-1 corepressor protein interacts and colocalizes with heterochromatin and euchromatic HP1 proteins: a potential factor for Kruppel-associated box zinc finger proteins in heterochromatin-mediated gene silencing. *Mol. Cell. Biol.* **19**, 4366–4378 (1999).
26. Brown, K. E. *et al.* Association of transcriptionally silent genes with Ikaros complexes at centromeric heterochromatin. *Cell* **91**, 845–854 (1997).
27. Murzina, N., Verreault, A., Laue, E. & Stillman, B. Heterochromatin dynamics in mouse cells: interaction between chromatin assembly factor 1 and HP1 proteins. *Mol. Cell* **4**, 529–540 (1999).
28. Taddei, A., Roche, D., Sibarita, J.-B., Turner, B. M. & Almouzni, G. Duplication and maintenance of heterochromatin domains. *J. Cell. Biol.* **147**, 1153–1166 (1999).
29. Cheung, P., Allis, C. D. & Sassone-Corsi, P. Signaling to chromatin through histone modifications. *Cell* **103**, 263–271 (2000).
30. Hecht, A., Laroche, T., Strahl-Bolsinger, S., Gasser, S. M. & Grunstein, M. Histone H3 and H4 N-termini interact with Sir3 and Sir4 proteins: a molecular model for the formation of heterochromatin in yeast. *Cell* **80**, 583–592 (1995).

**Acknowledgements**

We would like to thank M. Busslinger for the *Pax5* cDNA; P. B. Singh for the *HP1β* (*M31*) and *mPC1* (*M33*) cDNAs, and the *HP1β* antibodies; A. Verreault for the murine *HP1α* and *HP1γ* cDNAs; P. Chambon for *HP1α* antibodies; L. Huber for rabbit anti-Myc (9E10) antibodies; and Y. Zou for the MSCV–MIGR1 retroviral vectors. We acknowledge I. Gorny for help with peptide synthesis and M. Doyle for contributing to the *Suv39h2* knock-out. We are grateful to D. Allis for discussions and to M. Busslinger for comments and critical reading of the manuscript. Research in T.J.'s laboratory is supported by the IMP through Boehringer Ingelheim, the Austrian Research Promotion Fund and the Vienna Economy Promotion Fund.

Correspondence and requests for materials should be addressed to T.J. (e-mail: jenuwein@nt.imp.univie.ac.at).

**Selective recognition of methylated lysine 9 on histone H3 by the HP1 chromo domain**

Andrew J. Bannister\*†, Philip Zegerman\*†, Janet F. Partridge‡, Eric A. Miska\*, Jean O. Thomas§, Robin C. Allshire‡ & Tony Kouzarides\*

\* Wellcome/CRC Institute and Department of Pathology, University of Cambridge, Tennis Court Road, Cambridge CB2 1QR, UK  
 ‡ MRC Human Genetics Unit, Western General Hospital, Crewe Road, Edinburgh EH4 2XU, UK  
 § Department of Biochemistry, University of Cambridge, 80 Tennis Court Road, Cambridge CB2 1GA, UK  
 † These authors contributed equally to this work

Heterochromatin protein 1 (HP1) is localized at heterochromatin sites where it mediates gene silencing<sup>1,2</sup>. The chromo domain of HP1 is necessary for both targeting and transcriptional repression<sup>3,4</sup>. In the fission yeast *Schizosaccharomyces pombe*, the correct localization of Swi6 (the HP1 equivalent) depends on Clr4, a homologue of the mammalian SUV39H1 histone methylase<sup>5,6</sup>. Both Clr4 and SUV39H1 methylate specifically lysine 9 of histone H3 (ref. 6). Here we show that HP1 can bind with high affinity to histone H3 methylated at lysine 9 but not at lysine 4. The chromo domain of HP1 is identified as its methyl-lysine-binding domain. A point mutation in the chromo domain, which destroys the gene silencing activity of HP1 in *Drosophila*<sup>3</sup>, abolishes methyl-lysine-binding activity. Genetic and biochemical analysis in *S. pombe* shows that the methylase activity of Clr4 is necessary for the correct localization of Swi6 at centromeric heterochromatin and for gene silencing. These results provide a stepwise model for the formation of a transcriptionally silent heterochromatin: SUV39H1 places a ‘methyl marker’ on histone H3, which is then recognized by HP1 through its chromo domain. This model may also explain the stable inheritance of the heterochromatic state.

The histone code hypothesis predicts the existence of domains that specifically recognize modified histone residues<sup>7</sup>. One such domain is the bromodomain, which allows transcription factors such as P/CAF and TAF<sub>II</sub>250 to recognize histone tails only when they are acetylated at lysine residues<sup>8,9</sup>. To identify an equivalent domain that recognizes methyl-lysines, we examined a number of chromatin-associated factors for their ability to recognize specifically a histone H3 peptide (residues 1–16) tri-methylated at lysines 4 and 9.

Figure 1b shows that one protein, HP1, was able to bind to the methylated peptide (red line), but not to the unmethylated peptide (data not shown), using surface plasmon resonance (SPR) analysis. Other chromatin-associated proteins, such as Mi2, MeCP2 and P/CAF did not bind in this assay (data not shown). Of the two conserved domains in HP1 (Fig. 1a), the chromo domain was able to bind (Fig. 1b, green line) whereas the chromo-shadow domain was not (blue line). Figure 1c shows that the on-rate for the chromo domain (red line) is not affected by the addition of unmethylated histone H3 peptide (green line), but binding is completely abolished in the presence of the methylated H3 peptide (blue line). The dissociation constant (*K<sub>d</sub>*) of the HP1 chromo domain for the methylated H3 peptide (methyl-lysine) is about 70 nM, as determined by SPR (data not shown). The affinity of the HP1 chromo domain for methyl-lysine compares favourably with the affinity of the TAF<sub>II</sub>250 and P/CAF bromodomains for acetyl-lysine<sup>8</sup>, although a more definitive comparison will be possible with ITC analysis of the HP1/methyl-lysine interaction. Our analysis of other chromo domain proteins such as polycomb (M33), Mi2 and